

Fourier Analysis of Beamforming Data at the Tip of an Axial Fan Rotor

Bence Tóth^{1*}, János Vad¹

RESEARCH ARTICLE

Received 22 December 2015; accepted after revision 31 March 2016

Abstract

Axial fans operate in large numbers, often in the close vicinity of humans, therefore reducing their noise is a primary concern. In this paper, beamforming is applied to get information about the location and strength of noise sources on the rotor. This information is invaluable, however, difficult to interpret because of some limitations of the beamforming method. The broadband noise radiated in the upstream direction by an axial fan rotor has been examined by means of a phased array microphone system, and the recorded data have been processed with the use of the Rotating Source Identifier beamforming algorithm. In order to reduce the complexity of the source maps, spatial Fourier analysis has been applied to the beamforming-based circumferential source strength distribution taken at the tip radius of the rotor, where the complexity of the local aerodynamic phenomena makes the evaluation of the aeroacoustic noise source data especially challenging. As part of the processing method, a criterion has been introduced for identifying the significant components of the noise sources. The Fourier analysis enabled the effective enhancement of distinct noise sources out of the beamforming database, despite the presence of signal perturbations and limitations. The noise sources have been located and quantified with use of the Fourier transformation and with help of a criterion based on the physical properties of the noise generation mechanisms.

Keywords

axial fan, beamforming, Fourier analysis, noise reduction, phased array microphone

1 Introduction

Reducing the noise of axial fans is an important task because of the large numbers of such devices operating in the close vicinity of humans. In order to make turbomachinery quieter, the primary sources of noise have to be identified. The phased array microphone technique, supplemented by an appropriate beamforming algorithm, is a valuable tool that uses simultaneously recorded acoustic pressure signals to deliver information on the spatial distribution of noise sources [1, 2]. Using the Rotating Source Identifier (ROSI) [3] algorithm, beamforming can be applied to rotating objects, and spatial source distributions can be obtained e.g. for axial fan rotors. Using aerodynamic modelling, the located noise sources can be evaluated in association with aerodynamic phenomena occurring in the rotor. Thus, correlations can be sought between rotor aerodynamics and noise emission. Then, by modifying the geometry, one may be able to reduce noise. Such analysis is reported in [4, 5] suggesting simple design guidelines for noise reduction and efficiency improvement for axial fans. The present investigation, similarly to the aforementioned references, focuses on broadband noise sources.

While the spatial source distributions, often called beamform maps, contain invaluable information, their interpretation requires expertise and usually involves subjective judgments and decisions [6, 7]. One of the reasons for that is because beamform maps contain spurious peaks resulting from the presence of sidelobes [1, 8]. A larger source region may also pose the question whether it is a result of one, spatially extended source mechanism, or of multiple separate sources located close to each other [7], that the beamforming method is unable to resolve. This question arises because the beamforming algorithm, in itself, cannot make any distinction between noise sources of distinct physical origin: it detects the sum of the resultant noise. Making a distinction between noise sources is a task of the *processing method* of beamforming data. In this step, one possible criterion for making a distinction between multiple sources identified close to each other is the *theoretical resolution*.

The theoretical resolution, i.e. the theoretical limit distance of two sources that are just resolved, is usually defined through

¹ Department of Fluid Mechanics, Faculty of Mechanical Engineering, Budapest University of Technology and Economics, H-1111 Budapest, Bertalan Lajos Street 4-6, Hungary

* Corresponding author, e-mail: tothbence@ara.bme.hu

an optical analogy [9]. The Rayleigh and the Sparrow limit are often used [10], both of which define the smallest resolved distance as being proportional to the sensor size, and inversely proportional to the wavelength [10]. Each of these definitions contain a constant factor though, determined from arbitrary assumptions regarding the acuteness of the human eye [11]. Their direct application to acoustic source localization is therefore firstly doubtful (i.e. optical versus acoustic principle), and secondly, contains subjective elements originating from the arbitrarily chosen multipliers. Other resolution criteria exist, too, such as the *full width at half maximum* measure. But, even though this criterion does not include assumptions about human sight, it still defines resolution as the width of the beam at *half* the maximum value, again chosen arbitrarily.

It is not the intention of the authors to formulate new resolution criteria. Their aim is to analyse beamform maps, and decide whether a source region can be attributed to one mechanism or several ones. The authors wish to achieve that without using any of the aforementioned assumptions and subjective criteria that the optical resolution criteria include.

Therefore a new methodology is proposed, that does not require optics-based criteria, however, is still able to give information about sources that are located close to each other. The periodicity of the aerodynamic as well as aeroacoustic features of the rotor, originating from the repetition of the rotor blade passages, inspired the authors to apply spatial Fourier transform onto source strength distributions taken from the beamform map around the circumference of the fan. In the current study, only the tip radius was chosen to illustrate the effectiveness of the proposed method. This is because the most complex features of the beamform maps are found at the outermost part of each blade [4, 5], being in accordance with the complexity of the local aerodynamic phenomena. An example source map is shown in Fig. 1 to illustrate that. However, this choice of radius has no effect on the applicability of the method, as it can be used for any radius; it is just to illustrate the algorithm.

As the results will show, the representation of the source distribution in the spatial frequency domain is spectacularly simplified, enabling the introduction of a mathematically algorithmized and convenient data processing and source identification methodology. Due to this, effects in the spatial frequency domain can be interpreted in a clear and self-evident manner. The phase angle gives information about the source locations, while amplitudes at different spatial frequencies show the relative significance of various sound source mechanisms. Furthermore, these amplitude spectra provide a simple, objective and physically meaningful way to separate significant sources from beamform artefacts.

The aims of this paper are the following. First, to demonstrate the capabilities of spatial Fourier analysis via a case study. Second, to describe a mathematically established and algorithmized method for data filtering, processing, and evaluation that

is generally applicable for other beamforming investigations of rotors, or any periodic object. Last, to show the simultaneous evaluation of the amplitude and phase spectra, leading to localization and quantification of dominant noise sources on the selected blade radius.

To the authors' best knowledge, this is the first paper in which spatial Fourier analysis is applied onto beamforming data of axial fans.

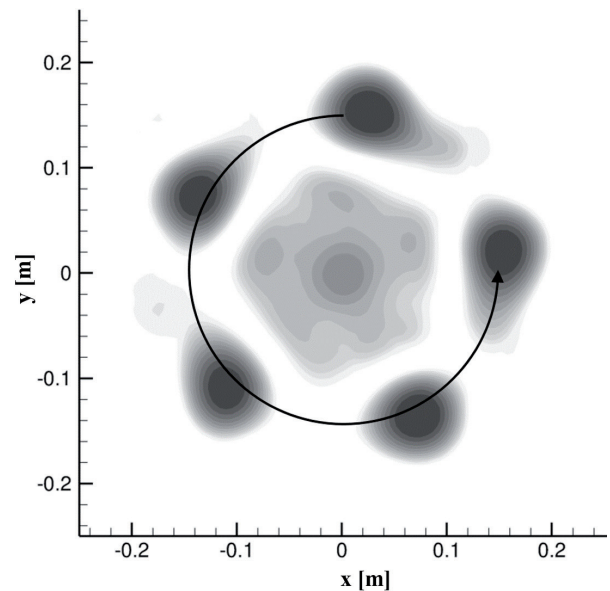


Fig. 1 Source map in the third-octave band centred on $f = 5000$ Hz. The darker colours indicate higher source strengths, while the arc shows the rotor tip radius.

2 Methodology

2.1 Beamforming

The ROSI method [3] is used herein for the investigation of rotating noise sources. The algorithm consists of two steps. First, the rotating target is placed into a co-rotating frame of reference. This is achieved, for all points of the beamform grid, by determining its location in time using the rotation speed, and its initial location, then calculating the propagation time delays between the point and each microphone for each time step. After that, the Doppler shift is removed from the recorded noise by interpolating the acoustic pressure signal onto a set of time points determined from the calculated propagation delays. Then *delay-and-sum* beamforming [1, 2] is carried out in the frequency domain to localize the sound sources. This means transforming the pressure signals into frequency domain, then adjusting their phases to account for different propagation time delays resulting from different source-to-microphone distances. In the process, the diagonal of the cross-spectrum matrix is removed to reduce the effect of uncorrelated measurement noise. By repeating the same procedure for all grid points, source maps can be created for each chosen frequency. For simpler evaluation, such source maps can be summed over specific frequency bands. In this study, third-octave bands are used.

These source maps represent the *source strength* of the detected noise from a certain reference distance. The source strength of a noise source at a given location, obtained by means of the beamforming technique, is in analogy with the *effective sound pressure* in acoustics.

2.2 Spatial Fourier transformation

Once the source maps for the third-octave bands under consideration are created, the source strength distribution is extracted from each of them at a prescribed radius – i.e. the blade tip radius in the present studies – as a function of the circumferential angle $\varphi = 0 \dots 2\pi$, using an equidistant spacing. The extraction path is shown in Fig. 1. Thus each distribution contains the source strengths encountered when going around the fan rotor. These extracted source strength distributions are denoted by $s_f(\varphi)$, where the index f indicates the mid-frequency of the third-octave band under discussion. Because of the expected strong spatial periodicity, each of these functions is decomposed into a sum of phase-shifted cosine functions according to the following formula:

$$s_f(\varphi) = \sum_{k=0} \tilde{A}_f(k) \cos(k(\varphi - \tilde{\beta}_f(k))) \quad (1)$$

The amplitude coefficients \tilde{A}_f and the phase angles $\tilde{\beta}_f$ are extracted from the discrete Fourier transformation of $s_f(\varphi)$. To avoid ambiguity at higher spatial frequencies, the smallest possible non-negative $\tilde{\beta}_f$ values are chosen.

Physically, the presence of the N fan blades is expected to be manifested in a strong periodicity of the sound sources, providing a way of their characterization. Therefore, it is useful to introduce a dimensionless spatial frequency having the following properties. $\phi = 0$ should express the temporal average (DC term) of the source strength around the circumference, while a positive integer ϕ should indicate how many times the chosen mode presents a peak *in each blade passage*. This behaviour is easily achieved by introducing ϕ in the following way:

$$\varphi = k/N. \quad (2)$$

Using this definition, the amplitude and phase can both be formulated as a function of ϕ :

$$A_f(\varphi) = \tilde{A}_f(\varphi/N), \quad (3)$$

$$\beta_f(\varphi) = \tilde{\beta}_f(\varphi/N). \quad (4)$$

This way, for each third-octave band, an amplitude spectrum $A_f(\phi)$ and a phase spectrum $\beta_f(\phi)$ is obtained defined at discrete values of $\phi = 0, 1/N, 2/N \dots$. Then $\phi = 1$ (at $k = N$) represents a single peak in each blade passage (i.e. N peaks over the entire circumferential angle range of $\varphi = 0 \dots 2\pi$). $\phi = 2$ (at $k = 2N$) represents two peaks in each blade passage, etc.

2.3 Significant peaks

The aim of the present modelling is to identify those significant peaks that are related to physical phenomena being characteristic periodically for each blade passage (numbered by the blade count N). For this purpose, peaks related to dimensionless spatial frequencies of $\phi = 1, 2, 3 \dots$ are to be considered.

In the modelling process described above, unintended physical effects that are *not* characteristic periodically for each passage, but only for a portion of them, appear as *perturbation*. Some non-exhaustive examples for such effects are as follows, being characterized by the ϕ values specified below.

- Violation in periodicity of the fan geometry, e.g. non-uniform tip clearance along the circumference, due to rotor eccentricity. This causes a circumferentially distributed non-uniformity in the noise, characterized by $\phi = 1/N$, since the tip clearance has a single minimum and maximum along the circumference.
- Violation in periodicity of the rotor blade geometry / blade loading, leading to a local amplification / moderation of noise. Depending on the number of irregular blades, this effect is characterized by $\phi = 1/N$ (a single blade of larger noise), $2/N$, (two blades), etc.

All of the aforementioned effects cause perturbation in modelling also at their harmonics.

Within a given third-octave band f , any peak at $\phi = 1, 2, 3 \dots$ is to be judged significant only if the amplitude of the related periodic signal exceeds the amplitude of the aforementioned perturbations. On this basis, the following criteria is proposed for identification of the significant peaks. In order to be considered significant, a peak must exceed a certain I_f limit in its third-octave band:

$$A_f(\varphi) > I_f. \quad (5)$$

This limit is the maximum perturbation amplitude, which is the maximum value out of the amplitudes occurring at the discrete spatial frequencies at which perturbation occurs, i.e. where ϕ is not an integer, as detailed above in the list:

$$I_f = \left\{ \max A_f \left(\frac{i}{N} \right) \middle| i = 1, 2, \dots, N-1 \right\} \quad (6)$$

Noise sources with significant peaks are then collected and classified according to the third-octave frequency in which they appear, and to their spatial frequency, i.e. how many times they cause a peak to appear per blade passage. In this way, the source maps can be characterized in an objective way using the least possible amount of data that still has the power to reveal important features of the underlying aeroacoustic phenomena.

This analysis has a further advantage of being able to deal with the question of separating sources. If there are more

important peaks in the vicinity of each other, they will show up in the harmonics of the spatial frequency. Then, depending on their magnitude relative to the noise floor in (6), they will be either classified as separate significant peaks, or will be neglected as side-effects. Therefore closely spaced sources are effectively dealt with even without applying resolution criteria.

The steps of the proposed analysis method are shown in Fig. 2 in the form of a flow chart.

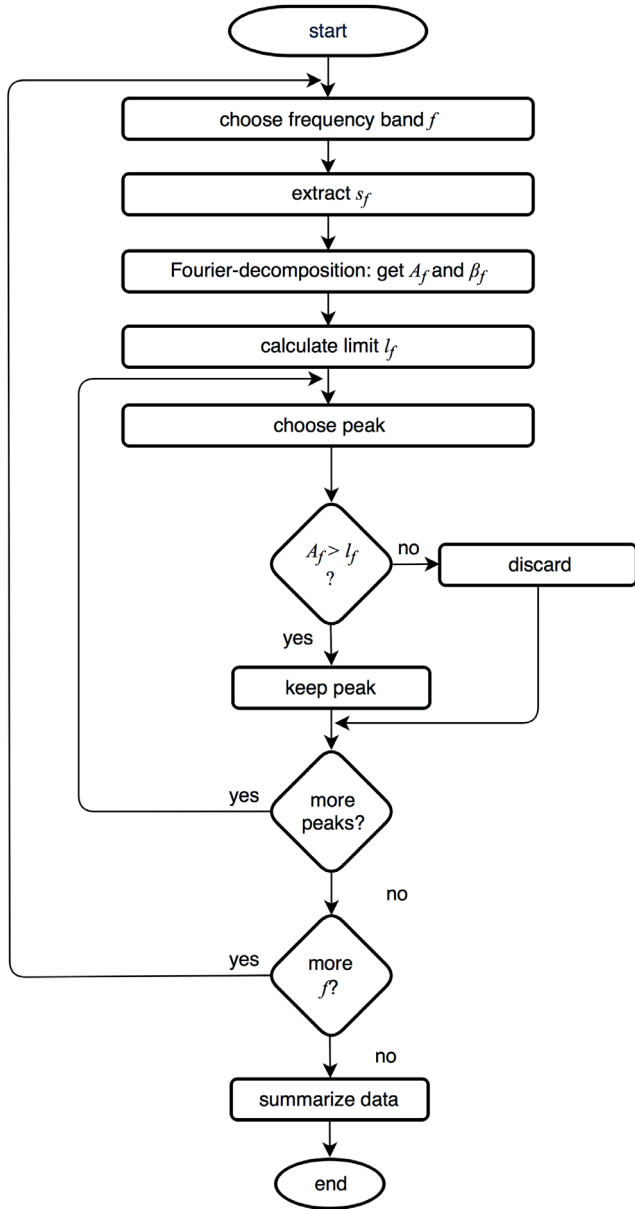


Fig. 2 Method flow chart

3 Case study

The proposed method is demonstrated in a case study, by applying it to measurements of an axial fan reported in [4, 5]. The case study fan has a one-stage rotor-only configuration with tip diameter $d_t = 0.3$ m, hub-to-tip diameter ratio $v = 0.3$, and frequency of rotation $n = 23.83$ Hz. This frequency was measured via an optical position transducer. Beamforming measurements are carried out on the upstream side using

an Array 24 (OptiNav, Inc., United States) phased array microphone and the accompanying signal processing equipment, from a distance of 0.5 m from the leading edge of the fan blades, with a sampling frequency of 44100 Hz applied throughout the 20 s data acquisition.

Measurements were processed using an in-house code based on the ROSI [3] algorithm. Narrowband source maps were created using a transform length of 1024. The appropriate narrowband maps were then summed to create third-octave band maps centred on 2000 Hz, 2500 Hz, 3150 Hz, 4000 Hz, 5000 Hz, and 6300 Hz. These bands were chosen because earlier research has shown that below the 2000 Hz band, no distinct sources can be identified due to the large wavelength, while above the 6300 Hz, the emitted noise of the fan is significantly reduced [12].

The circumferential distribution $s_f(\phi)$ taken at the tip diameter for each investigated third-octave band is shown in Fig. 3 with solid lines.

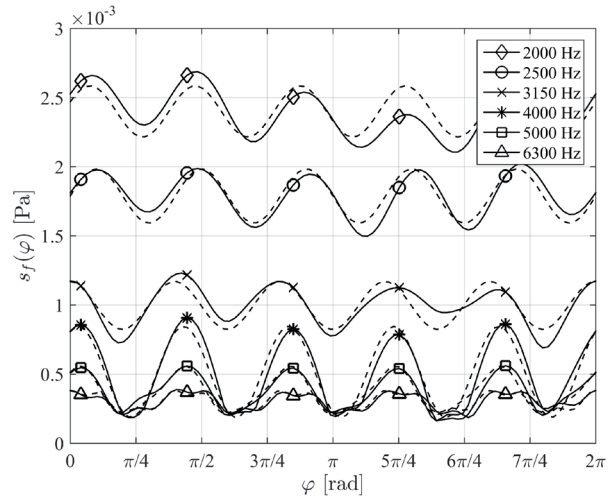


Fig. 3 Measured (solid) and reconstructed (dashed) distributions of source strength around the circumference of the fan in the analysed third-octave bands

Each of these functions is transformed into the spatial frequency domain. The magnitude of a spatial frequency spectra (for the third-octave band around 5000 Hz) is shown as an example in Fig. 4. The figure shows that a very large average (DC) value is present in the signal ($\phi = 0$), a relatively large value occurs at the spatial frequency of the blading ($\phi = 1$), then smaller peaks appear at integer multiples of this base frequency. Furthermore, there is some noise at the frequencies between the aforementioned peaks, with their magnitude being between that of the peak at $\phi = 2$ and the peak at $\phi = 3$. The amplitude spectra are dominated by only a few peaks. Therefore, the signals presented in Fig. 3 can be reasonably well approximated using a low number of Fourier components. Here the criterion of Eqs. (5) to (6) is applied to determine the limit amplitude, below which the Fourier components are

neglected. The horizontal solid line indicates this limit in the example in Fig. 4, above which only three components remain to be considered as significant components: the average at $\phi = 0$, as well as the peaks related to $\phi = 1$ and $\phi = 2$.

The other frequency bands have a similar behaviour. After applying the criterion for the significant peaks, the average value ($\phi = 0$) and the component with the periodicity of the blade count ($\phi = 1$) is considered at all frequencies as significant. Furthermore, the aforementioned significant component at 5000 Hz appears at $\phi = 2$ (conf. Fig. 4). Finally, one additional significant component appears at 6300 Hz at $\phi = 3$. Besides these, no significant components are identified.

The spatial frequency spectrum shown in Fig. 4 is quite discretized. This is because the circumferential source strength distributions were extracted by interpolating the rectangular beamform grid onto a circular grid. Therefore the original number of grid points defines the number of samples used for the Fourier transform, and as such, the smoothness of the spatial frequency spectra.

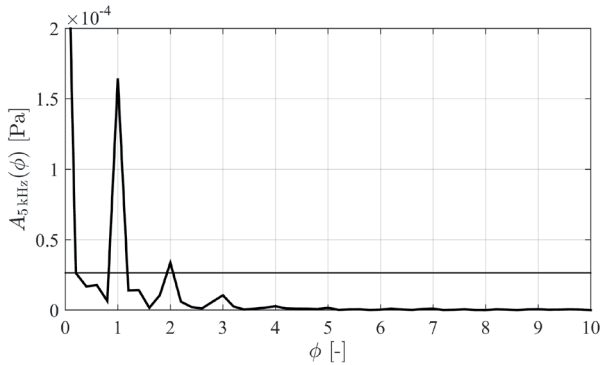


Fig. 4 Amplitude spectrum as a function of dimensionless spatial frequency in the third-octave band centred on $f = 5000$ Hz

To judge how good this representation is, Fig. 3 shows the source strength distributions reconstructed with use of only the significant Fourier components (dashed lines) together with the measured data (solid lines). The functions are in good agreement, as it can be seen from the figure. To show that numerically as well, the root mean square deviation of the reconstructed and the measured signals were calculated and normalized by the range of the data. This value is about 0.17 for the lowest band, while for all the other bands, it is below 0.13, again indicating a good agreement.

In the range of the investigated third-octave bands, the spatial resolution of the beamforming process allows for the identification of finer details. As such, the periodicity expected from the periodic blade pattern is clearly visible. At higher frequencies, the agreement is even better: the spatial variation is very well captured and recovered even from just three modes. This illustrates the usefulness of the proposed Fourier-based spatial filtering technique that can represent source strength distributions with only a few harmonic components. Up to 4000 Hz,

only the average and the N -periodic component, then at 5000 Hz the average, the N -periodic and the $2N$ -periodic, while at 6300 Hz just the average, the N -periodic and the $3N$ -periodic components are necessary.

The acquired data on the significant peaks are summarized in Table 1. The phase angles have been obtained from the Fourier phase spectra of the signals.

The peak ID consists of the third-octave band mid-frequency in Hz, then the normalized spatial frequency ϕ , and finally, the serial number of the peak going from one to ϕ . The latter data is used in further evaluation of the results.

Table 1 Significant peaks: ID, amplitude and angular location

Peak ID	$A \cdot 10^{-5}$ [Pa]	Phase β [deg]
2000/1/1	18.51	16.12
2500/1/1	19.56	20.53
3150/1/1	17.35	2.15
4000/1/1	32.90	8.17
5000/1/1	16.45	6.88
5000/2/1	3.37	13.03
5000/2/2	3.37	49.03
6300/1/1	7.48	10.16
6300/3/1	2.63	0.00
6300/3/2	2.63	24.00
6300/3/3	2.63	48.00

The phase angles, i.e. the angular locations of the significant peaks inside a blade passage are shown in Fig. 5. When creating this figure, the periodicity as well as the multiplicity of the peaks at higher spatial frequencies was taken into account. That means the figure shows *each* angle at which a significant Fourier component has a maximum (it is not only the angle corresponding to the first occurrence that is presented). The phase on the vertical axis has been normalized by the angular extent of one blade passage, $2\pi/N$. This way, the maximum angle is 1, while the angle difference between repeating peaks at higher ϕ values is $1/\phi$. A constant phase shift has been applied to each data point in Fig. 5, to set the minimum angle (related to the 6300/1/1 peak) to zero, for a better overall representation of the relative positions of the peaks.

It can be seen that the source strength peaks of $\phi = 1$ are located close to each other. At $\phi = 2$, the only significant component is in the third-octave band centred on 5000 Hz. This means two peaks in each blade passage: one at an angle similar to the peak at $\phi = 1$, and another one that is half a period away. At $\phi = 3$, only the third-octave band centred on 6300 Hz contains significant source strength. The first peak appears at zero angle, while the other two follow with shifts of $1/3$.

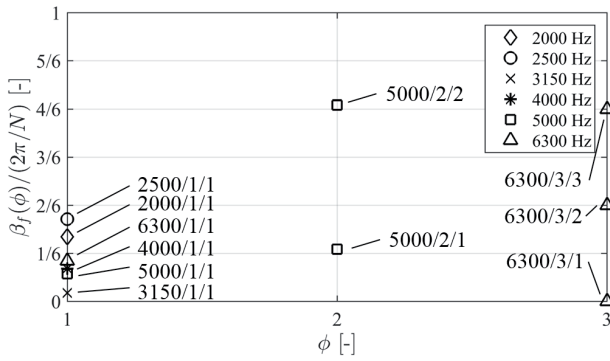


Fig. 5 Angular location of significant peaks inside a blade passage

4 Conclusion

The paper has dealt with noise sources obtained from phased array measurements on axial fans. The periodicity of the rotor suggested the application of spatial Fourier transform on the circumferential source strength distributions. This was carried out at the blade tip radius for several third-octave bands. The results show that in this way the sources can be represented in a comprehensive manner. Amplitudes and peak locations can be identified belonging to various spatial frequencies. Furthermore, a natural and physically sensible criterion is given to determine whether a peak in the amplitude spectrum can be considered significant. This allows the reduction of beamform data and the removal of measurement artefacts. At the end, a set of significant peaks are obtained, with their temporal frequencies, spatial frequencies, amplitudes and angular locations. This representation may simplify further investigations, e.g. noise reduction by fan blade redesign, in which case for each new geometry, it would be enough to compare the amplitudes of the known peaks to the original ones to judge the outcome of the modifications.

The case study presented herein is considered as a starting point for a generally applicable, algorithmized methodology for evaluation of beamforming data on axial fan noise via the Fourier analysis. The further development and generalization of the methodology is the subject of further research.

Nomenclature

Abbreviations

ROSI Rotating Source Identifier

Latin letters

A Fourier amplitude of source strength [Pa]
 d diameter [m]
 f (temporal) mid-frequency of third-octave band [Hz]
 i running index [-]
 k mode number [-]
 l amplitude limit [Pa]
 n speed of rotation [rad/s]

N number of fan blades [1]
 s source strength distribution [Pa]
 x source map horizontal coordinate [m]
 y source map vertical coordinate [m]

Greek letters

β Fourier phase angle of source strength [rad]
 φ circumferential angle [rad]
 ϕ normalized spatial frequency [1]
 ν hub-to-tip ratio [1]

Subscripts

f third-octave band mid-frequency index
 t rotor tip

Others

\sim indicates a function of k mode number

Acknowledgements

This work has been supported by the Hungarian National Fund for Science and Research under contract No. OTKA K 112277.

The work relates to the scientific programs “Development of quality-oriented and harmonized R+D+I strategy and the functional model at BME” (Project ID: TÁMOP-4.2.1/B-09/1/KMR-2010-0002) and “Talent care and cultivation in the scientific workshops of BME” (Project ID: TÁMOP-4.2.2/B-10/1-2010-0009).

References

- [1] Dougherty, R. P. "Beamforming in acoustic testing." In: *Experimental Aeroacoustics*. (Mueller, T. J. (ed.)), pp. 62-97, Springer, Berlin, 2002. DOI: [10.1007/978-3-662-05058-3](https://doi.org/10.1007/978-3-662-05058-3)
- [2] Koop, L. "Beam forming methods in microphone array measurements." In: *VKI Experimental Aeroacoustics*. (Riethmuller, M. L., Lena, M. R. (ed.)), von Karman Institute for Fluid Dynamics, Rhode Saint Genèse, 2006.
- [3] Sijtsma, P., Oerlemans, S., Holthusen, H. "Location of rotating sources by phased array measurements." In: *Proceedings of the 7th AIAA/CEAS Aeroacoustics Conference*, Maastricht, 2001. DOI: [10.2514/6.2001-2167](https://doi.org/10.2514/6.2001-2167)
- [4] Benedek, T., Vad, J. "Spatially Resolved Acoustic and Aerodynamic Studies Upstream and Downstream of an Industrial Axial Fan with Involvement of the Phased Array Microphone Technique." In: *Proceedings of the European Turbomachinery Conference (ETC'15)*, Madrid, 2015.
- [5] Benedek, T., Vad, J. "An industrial on-site methodology for combined acoustic-aerodynamic diagnostics of axial fans, involving the Phased Array Microphone technique." *International Journal of Aeroacoustics*. 2016. DOI: [10.1177/1475472X16630849](https://doi.org/10.1177/1475472X16630849)
- [6] Sarraj, E., Schulze, C., Zeibig, A. "Aspects of source separation in beamforming." In: *Proceedings of the Berlin Beamforming Conference*, Berlin, 2006.
- [7] Tóth, B., Vad, J. "Challenges in evaluating beamforming measurements on an industrial jet fan." In: *Proceedings of the Conference on Modelling Fluid Flow (CMFF'15)*, Budapest, 2015.

- [8] Dougherty, R. P. "Functional beamforming." In: *Proceedings of the 20th AIAA/CEAS Aeroacoustics Conference*, Atlanta, 2014. DOI: [10.2514/6.2014-3066](https://doi.org/10.2514/6.2014-3066)
- [9] Hald, J., Christensen, J. J. "Beamforming." *Brüel&Kjaer Technical Review*, Vol. 1, 2004.
- [10] Dougherty, R. P., Ramachandran, R. C., Raman, G. "Deconvolution of sources in aeroacoustic images from phased microphone arrays using linear programming." *International Journal of Aeroacoustics*. 12(7-8), pp. 699-717. 2013. DOI: [10.1260/1475-472X.12.7-8.699](https://doi.org/10.1260/1475-472X.12.7-8.699)
- [11] Jenkins, F. A., White, W. E. "*Fundamentals of Optics*." 4th Edition. McGraw-Hill Primis Custom Publishing, New York, 1976.
- [12] Benedek, T., Vad, J. "Concerted Aerodynamic and Acoustic Diagnostics of an Axial Flow Industrial Fan, Involving the Phased Array Microphone Technique." Paper GT2014-25916, In: *Proceedings of the ASME Turbo Expo 2014*, Düsseldorf, 2014. DOI: [10.1115/GT2014-25916](https://doi.org/10.1115/GT2014-25916)